Appl. Math. and Comp. Sci., 1996, vol.6, No.2, 207–221

MATHEMATICAL MODELLING AND NUMERICAL SIMULATION OF INDUCTION HEATING PROCESSES†

JACQUES RAPPAZ*, MAREK ŚWIERKOSZ*

This paper deals with numerical simulation of induction heating for tri-dimensional time-varying axisymmetric geometries. A mathematical model is presented together with the numerical scheme used to solve it. The whole is illustrated by results of sample computations.

1. Introduction

Induction heating is widely used in industrial processes involving heat treatment, such as quenching, brasing, preheating for forging operations, coating of surfaces, melting or stirring in electromagnetic crucibles. It involves both electromagnetic and thermal phenomena, described by coupled non-linear partial differential equations.

The essential components of an induction heating setup are one or more inductors and one or several metallic workpieces to be heated (Fig. 1). In most industrial processes, the inductors move with respect to the workpieces. This is an essential characteristic of quenching treatment and of most processes involving a production line. The inductors are supplied with alternating current. The frequencies used range from a thousand to several hundred thousand cycles per second.

The current flowing through the inductors generates a rapidly oscillating magnetic field. This in turn induces the so-called eddy currents in the workpiece. Due to the Joule effect and, in some cases, also to the hysteresis effect, these currents produce heat inside the workpiece. It is worth noticing that in most practical cases, most heat is generated in a shallow layer below the surface of the workpiece. In fact, the eddy current intensity decreases exponentially with the distance from the surface. This phenomenon is known as the skin effect.

In this research, we considered induction heating setups which present an axial symmetry. The aim was to obtain a model permitting efficient numerical simulations that could be used for the design and optimization of induction heating plants. It was assumed that the coils were supplied with sinusoidal alternating current, so as to obtain a steady-state electromagnetic problem. The total voltage in each coil v_k and the angular frequency ω were considered to be given. Under these assumptions, we

† This research was supported by the Swiss "Nationaler Energie–Forschungs–Fonds" and performed in collaboration with the company Amysa Yverdon SA, Switzerland.

* Department of Mathematics, Swiss Federal Institute of Technology, CH–1015 Lausanne, Switzerland, e-mail: marek@dma.epfl.ch

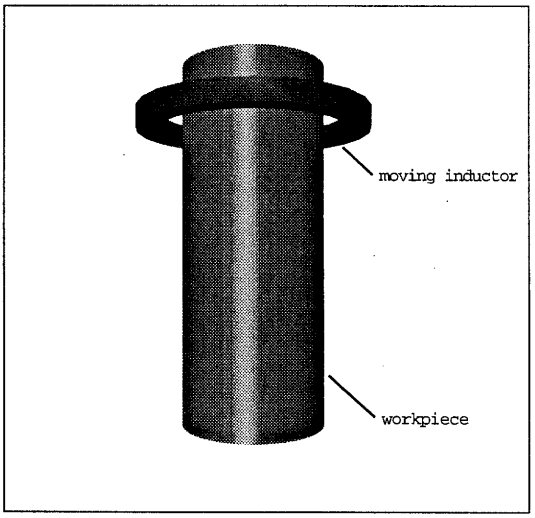

Fig. 1. A sample induction heating setup.

developed a mathematical model and a numerical scheme which gave rise to an eddy-current simulation package. This software was coupled with a heat equation solver and a microstructure computation module. We thus obtained a complete induction heating simulation code which is now used in industrial practice.

The paper is organized as follows. In Section 2, we describe the mathematical eddy-current model. Section 3 is devoted to the numerical scheme used to compute the solution to the model. Section 4 deals with the issue of simulating energetic effects of hysteresis phenomena. In Section 5, we present shortly the other physical models used and discuss briefly how they interact in the whole numerical simulation scheme. Finally, in Section 6, sample numerical results are presented and compared with experimental measurements.

2. Mathematical Eddy-Current Model

Let us consider an axisymmetric induction heating setup consisting of N conductors, i.e. inductors and workpieces. Let Δ_i, $i = 1,\ldots,N$, be N bounded open sets of $\mathbb{R}^3$ corresponding to the areas in space occupied by the conductors. These sets are obtained by revolution of N open simply-connected sets $\Omega_i \subset \mathbb{R}^2$, $i = 1,\ldots,N$, around a straight line that we consider to be the Oz axis of a Cartesian coordinate system (x,y,z). Let us denote by Δ the union of the sets Δ_i: $\Delta = \cup_{i=0}^{N}\Delta_i$, by Ω the union of the sets Ω_i: $\Omega = \cup_{i=0}^{N}\Omega_i$, and by Δ' the complement of $\overline{\Delta}$ in $\mathbb{R}^3$ ($\overline{\Delta}$ denotes the closure of Δ). We order the sets Δ_i in such a way that $\Delta_1, \Delta_2, \ldots, \Delta_r$ correspond to the inductors while $\Delta_{r+1}, \ldots, \Delta_N$ correspond to the workpieces. The sets $\Delta_1, \Delta_2, \ldots, \Delta_r$ are not simply-connected and therefore have necessarily a toroidal geometry.

We start building our model from Maxwell equations with displacement currents neglected, and the Ohm law. The following equations hold in $\mathbb{R}^3$:

$$\operatorname{div} \mathbf{B} = 0 \tag{1}$$

$$\mathbf{curl}\, \mathbf{E} = -\frac{\partial \mathbf{B}}{\partial t} \tag{2}$$

$$\mathbf{curl}\, \mathbf{H} = \mathbf{j} \tag{3}$$

$$\nu \mathbf{B} = \mathbf{H} \tag{4}$$

Moreover, in the domain Δ, the Ohm law can be written as

$$\mathbf{j} = \sigma \mathbf{E} \tag{5}$$

Here t denotes time, $\mathbf{E}$ the electric field, $\mathbf{H}$ the magnetic field, $\mathbf{B}$ the magnetic induction, $\mathbf{j}$ the electric current density, σ the electric conductivity, and ν the magnetic reluctivity, i.e. the inverse of the magnetic permeability μ. For the moment, we assume that the values of σ, μ and ν do not depend on time. In reality, they will usually vary with temperature and, to a certain extent, with the magnetic field.

Let us consider now a cylindrical coordinate system (r, θ, z) with its associated natural tangent reference system $(\mathbf{e}_r, \mathbf{e}_\theta, \mathbf{e}_z)$. The Oz axis of this system is the same as the Oz axis of the Cartesian coordinate system considered before, i.e. it coincides with the symmetry axis of the setup. The following assumptions are made:

1. The fields $\mathbf{B}$, $\mathbf{H}$, $\mathbf{E}$ are such that their components in the reference system $(\mathbf{e}_r, \mathbf{e}_\theta, \mathbf{e}_z)$ do not depend on θ.
2. The electric current density is of the form $\mathbf{j} = j(r,z)e^{i\omega t}\mathbf{e}_\theta$, where $j : (r,z) \in \mathbb{R}^+ \times \mathbb{R} \mapsto j(r,z) \in \mathbb{C}$ is some complex-valued function.

It will also be assumed that there are no surface currents, i.e. no Dirac δ-like current "concentration" on the surface of the conductors.

Suppose that a periodic voltage of the form $v_k e^{i\omega t}$ (with v_k possibly equal to zero) is imposed in the sets Δ_k, $k = 1, \ldots, r$, which correspond to the inductor coils. In the sets Δ_k, $k = 1, \ldots, r+1$, we shall set $v_k \equiv 0$ by convention. Due to the linearity of the problem (with constant coefficients σ, μ and ν), we can look for the fields $\mathbf{B}$, $\mathbf{H}$, $\mathbf{E}$ in the form

$$\mathbf{B} = \Big(B_r(r,z)\mathbf{e}_r + B_\theta(r,z)\mathbf{e}_\theta + B_z(r,z)\mathbf{e}_z\Big)e^{i\omega t} \tag{6}$$

$$\mathbf{H} = \Big(H_r(r,z)\mathbf{e}_r + H_\theta(r,z)\mathbf{e}_\theta + H_z(r,z)\mathbf{e}_z\Big)e^{i\omega t} \tag{7}$$

$$\mathbf{E} = \Big(E_r(r,z)\mathbf{e}_r + E_\theta(r,z)\mathbf{e}_\theta + E_z(r,z)\mathbf{e}_z\Big)e^{i\omega t} \tag{8}$$

Here $B_r(r,z)$, $B_\theta(r,z)$, $B_z(r,z)$, $H_r(r,z)$, $H_\theta(r,z)$, $H_z(r,z)$, $E_r(r,z)$, $E_\theta(r,z)$, $E_z(r,z)$ are complex-valued functions to be determined. In the sequel, we shall omit the term $e^{i\omega t}$.

Our aim is now to show that under the above assumptions, the magnetic induction $\mathbf{B}$ can be expressed in terms of a scalar potential

$$\phi : (r,z) \in \mathbb{R}^+ \times \mathbb{R} \mapsto \phi(r,z) \in \mathbb{C} \tag{9}$$

Let us consider eqn. (3) expressed in cylindrical coordinates. Using (7) and Assumption 2, we get from (3) that

$$\left(-\frac{\partial H_\theta}{\partial z}\right)\mathbf{e}_r - \left(\frac{\partial H_z}{\partial r} - \frac{\partial H_r}{\partial z}\right)\mathbf{e}_\theta + \left(\frac{1}{r}\frac{\partial (rH_\theta)}{\partial r}\right)\mathbf{e}_z = j\mathbf{e}_\theta \tag{10}$$

which is equivalent to the system

$$-\frac{\partial H_\theta}{\partial z} = 0 \tag{11}$$

$$-\frac{\partial H_z}{\partial r} + \frac{\partial H_r}{\partial z} = j \tag{12}$$

$$\frac{1}{r}\frac{\partial (rH_\theta)}{\partial r} = 0 \tag{13}$$

Equation (11) implies that $H_\theta = H_\theta(r)$, and from (13) we get $H_\theta = \frac{c}{r}$, where c is a constant. If c were non-zero, we would have $\lim_{r\to 0} H_\theta = \infty$, which is absurd. Therefore, the magnetic field $\mathbf{H}$ has the form

$$\mathbf{H} = H_r(r,z)\mathbf{e}_r + H_z(r,z)\mathbf{e}_z \tag{14}$$

This result and eqn. (4) imply that the magnetic induction $\mathbf{B}$ also has the form

$$\mathbf{B} = B_r(r,z)\mathbf{e}_r + B_z(r,z)\mathbf{e}_z \tag{15}$$

Thus equation (1) yields

$$\frac{\partial}{\partial r}(rB_r) + \frac{\partial}{\partial z}(rB_z) = 0 \tag{16}$$

Equation (16) states the fact that the field $(r,z) \in \mathbb{R}^+ \times \mathbb{R} \mapsto (rB_r, rB_z) \in \mathbb{C}^2$ is divergence–free when we consider (r,z) as Cartesian coordinates. A well-known result (see e.g. the book by Dautray and Lions (1988)) allows us to conclude that this field can be expressed in terms of the curl of a scalar function. In other words, there exists a function $\psi : (r,z) \in \mathbb{R}^+ \times \mathbb{R} \mapsto \psi(r,z) \in \mathbb{C}$ such that

$$rB_r = -\frac{\partial \psi}{\partial z}, \qquad rB_z = \frac{\partial \psi}{\partial r} \tag{17}$$

Let $\phi : (r,z) \in \mathbb{R}^+ \times \mathbb{R} \mapsto \phi(r,z) \in \mathbb{C}$ be defined by $\phi(r,z) = \frac{1}{r}\psi(r,z)$. Equations (17) can then be rewritten in the form

$$B_r = -\frac{\partial \phi}{\partial z}, \qquad B_z = \frac{1}{r}\frac{\partial (r\phi)}{\partial r} \tag{18}$$

We conclude that there exists a vector magnetic potential $\mathbf{A}$ of the form

$$\mathbf{A}(r,z) = \phi(r,z)\mathbf{e}_\theta \tag{19}$$

such that

$$\mathbf{B} = \mathbf{curl}\,\mathbf{A} \tag{20}$$

Moreover, we clearly have

$$\operatorname{div}\mathbf{A} = 0 \tag{21}$$

since $\operatorname{div}\mathbf{A} = \dfrac{1}{r}\dfrac{\partial\phi}{\partial\theta}$. Using the Biot-Savart law, one can show that $\mathbf{B} \sim \dfrac{1}{(r^2+z^2)^{\frac{3}{2}}}$ as $(r^2+z^2)^{\frac{1}{2}} \to \infty$. In (17), ψ is defined up to a constant. Consequently, ϕ can be chosen so that $\phi \sim \dfrac{1}{r^2+z^2}$ as $(r^2+z^2)^{\frac{1}{2}}$ tends to infinity, or, in other words,

$$\phi = O\left(\frac{1}{r^2+z^2}\right) \quad \text{as} \quad |r|+|z| \to \infty \tag{22}$$

Taking into account (20), (4) and Assumption 2, eqn. (3) yields

$$\mathbf{curl}\,(\nu\,\mathbf{curl}\,\mathbf{A}) = j\mathbf{e}_\theta \tag{23}$$

which can be expanded to the form

$$-\left(\frac{\partial}{\partial r}\left(\frac{\nu}{r}\frac{\partial(r\phi)}{\partial r}\right)+\frac{\partial}{\partial z}\left(\nu\frac{\partial\phi}{\partial z}\right)\right)\mathbf{e}_\theta = j\mathbf{e}_\theta \tag{24}$$

This result holds both inside the conductors and outside them.

Outside the conductors, j is zero and ν is constant, so that (24) yields

$$\frac{\partial}{\partial r}\left(\frac{1}{r}\frac{\partial(r\phi)}{\partial r}\right)+\frac{\partial^2\phi}{\partial z^2} = 0 \tag{25}$$

This equation does not imply $\Delta\phi = 0$. However, multiplying it by $\sin\theta$, we get

$$\Delta(\phi\sin\theta) = 0 \tag{26}$$

So far, we have expressed the magnetic field and the magnetic induction in terms of a scalar magnetic potential ϕ. Our aim is now to find a relationship between the current density j, the potential ϕ, and the voltage v_k imposed on the conductor.

From the Ohm law (5) and Assumption 2, we get that $\mathbf{E} = E(r,z)\mathbf{e}_\theta$ in each open set Δ_k (corresponding to the location of a conductor). By rewriting eqn. (2) in cylindrical coordinates, taking into account (6) and (15), we get

$$i\omega(B_r\mathbf{e}_r + B_z\mathbf{e}_z)+\left(-\frac{\partial E}{\partial z}\right)\mathbf{e}_r+\left(\frac{1}{r}\frac{\partial(rE)}{\partial r}\right)\mathbf{e}_z = 0 \tag{27}$$

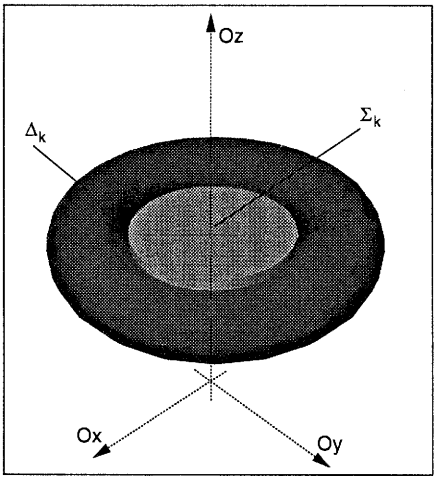

Fig. 2. Application of a voltage to a toroidal conductor.

i.e. $i\omega B_r = \dfrac{\partial E}{\partial z}$, $i\omega B_z = -\dfrac{1}{r}\dfrac{\partial (rE)}{\partial r}$. Substituting (18) into these equations, we get

$$-i\omega \frac{\partial \phi}{\partial z} = \frac{\partial E}{\partial z} \tag{28}$$

$$\frac{1}{r} i\omega \frac{\partial (r\phi)}{\partial r} = -\frac{1}{r}\frac{\partial (rE)}{\partial r} \tag{29}$$

or, equivalently,

$$\frac{\partial}{\partial z}(rE + i\omega r\phi) = 0, \qquad \frac{\partial}{\partial r}(rE + i\omega r\phi) = 0 \tag{30}$$

Consequently, there exist constants $c_k \in \mathbb{C}$, $k = 0, \ldots, N$, such that

$$rE + i\omega r\phi = c_k \quad \text{in } \Delta_k, \quad k = 0, \ldots, N \tag{31}$$

The Ohm law (5) yields

$$j = \sigma \left(-i\omega\phi + \frac{c_k}{r}\right), \qquad k = 1, \ldots, N \tag{32}$$

Now, for every non-simply-connected toroidal conductor Δ_k, there exists a disk Σ_k, centered on the Oz axis of the cylindrical coordinates system and orthogonal to this axis, such that the $\Delta_k \cup \Sigma_k$ is simply-connected (Fig. 2). The voltage v_k is then defined as a line integral of $\mathbf{E} + i\omega\mathbf{A}$ along $\partial\Sigma_k$. Since $\mathbf{A}$ takes the form (19), we get

$$v_k = \int_{\partial\Sigma_k} (E + i\omega\phi)\, \mathbf{e}_\theta \, \mathrm{d}\tau \tag{33}$$

Taking into account (31) and the fact that $\mathbf{d}\tau = \mathbf{e}_\theta r\,\mathrm{d}\theta$ in this case, we obtain

$$v_k = \int_0^{2\pi} c_k\,\mathrm{d}\theta = 2\pi c_k \tag{34}$$

Therefore, in any non-simply-connected set Δ_k, we have

$$j = \sigma\left(-i\omega\phi + \frac{v_k}{2\pi r}\right) \tag{35}$$

Any simply-connected axisymmetric set must have a non-empty intersection with the Oz axis, where r is zero. Since the current density cannot be infinite, eqn. (32) implies that c_k is zero in those of the sets Δ_k that are simply-connected.

Let us remark that an inductor cannot be simply-connected. In all workpieces, the voltage v_k is zero, which implies that c_k is zero also in those workpieces that are not simply-connected.

Equations (35), (24) and Assumption 2 yield the following condition, valid in any conductor Δ_k:

$$-\left(\frac{\partial}{\partial r}\left(\frac{\nu}{r}\frac{\partial(r\phi)}{\partial r}\right) + \frac{\partial}{\partial z}\left(\frac{\nu}{r}\frac{\partial(r\phi)}{\partial z}\right)\right) + i\omega\sigma\phi = \frac{\sigma v_k}{2\pi r} \tag{36}$$

We shall now attempt to find conditions on the boundary of the conductors. Let $[f]$ denote the jump of a function f on $\partial\Delta$, and let $\mathbf{n} = n_r\mathbf{e}_r + n_z\mathbf{e}_z$ be the unit vector normal to $\partial\Delta$. Equations (19) and (20) imply that ϕ must be continuous. Since we assume that there are no surface currents, we have

$$[\mathbf{H}\times\mathbf{n}] = 0 \tag{37}$$

on $\partial\Delta$. As $\mathbf{H}\times\mathbf{n} = (H_z n_r - H_r n_z)\mathbf{e}_\theta$, we get

$$[H_r n_z - H_z n_r] = 0 \tag{38}$$

Equations (18) and (4) yield

$$\left[\frac{\nu}{r}\left(\frac{\partial(r\phi)}{\partial z}n_z + \frac{\partial(r\phi)}{\partial r}n_r\right)\right] = 0 \tag{39}$$

or briefly $\left[\dfrac{\nu}{r}\dfrac{\partial(r\phi)}{\partial n}\right] = 0$. We thus have the following interface conditions:

$$[\phi] = \left[\frac{\nu}{r}\frac{\partial(r\phi)}{\partial n}\right] = 0 \tag{40}$$

Consequently, the model consists of eqn. (25) (or (26)) in Δ' (outside the conductors), eqn. (36) in Δ (inside the conductors), interface conditions (40) and the condition (22) at infinity.

3. Computation of the Eddy Currents

Our aim is now to formulate a set of equations that could be used in a numerical simulation code. The difficulty arises on account of the fact that eqn. (25) is defined over an unbounded domain. Therefore a straightforward solution by the finite-element method is not possible.

Equation (25) could be solved over the whole unbounded domain using the so-called "infinite elements". Another common way of dealing with such problems is to approach the infinite domain by a "sufficiently large" finite one, with suitable conditions on the boundary, and to solve the whole problem by the standard finite-element method.

In our case, these two solutions do not seem to be adequate. In fact, the assumption is that inductors may move with respect to the workpieces. Therefore, the mesh outside the conductors would have to vary with the inductor movement. Apart from other considerations, the generation of such a mesh would lead to efficiency problems.

We thus opted for a boundary-element-finite-element formulation. The behaviour of the magnetic potential outside the conductors will be expressed in terms of integrals over their boundary, while a classical finite-element formulation was chosen for the inside of the conductors.

The key of the boundary-element part is the so-called simple-double layer formulation. Let $G(y,x) = \dfrac{1}{4\pi|x-y|}$ denote the Green kernel in $\mathbb{R}^3$. Let f denote any function of $C^2(\mathbb{R}^3)$, harmonic in Δ' and such that $f = O\left(\dfrac{1}{|x|}\right)$ as $|x| \to \infty$. Then the value of f at any point $y \in \partial\Delta$ is given by the equation (Nédélec, 1977)

$$\frac{f(y)}{2} = \int_{\partial\Delta} \frac{\partial f(x)}{\partial n_x} G(y,x)\, \mathrm{d}s_x - \int_{\partial\Delta} \frac{\partial G(y,x)}{\partial n_x} f(x)\, \mathrm{d}s_x \tag{41}$$

where $\mathbf{n}_x$ denotes the unit vector normal to $\partial\Delta$ at the point x, oriented to the outside of Δ'.

We apply the above formulation to the function $\phi \sin\theta$ which satisfies eqn. (26). Let the points $x, y \in \mathbb{R}^3$ be respectively denoted by $x = (r,\theta,z)$, $y = (r_b,\theta_b,z_b)$ in cylindrical coordinates. Then the Green kernel is

$$G(r_b,\theta_b,z_b,r,\theta,z)$$

$$= \frac{1}{4\pi} \frac{1}{[(r_b\cos\theta_b - r\cos\theta)^2 + (r_b\sin\theta_b - r\sin\theta)^2 + (z_b - z)^2]^{1/2}} \tag{42}$$

Since the vector normal to $\partial\Delta$ has no component along $\mathbf{e}_\theta$, we have $\dfrac{\partial(\sin\theta)}{\partial n_x} = 0$.

Therefore eqn. (41) takes the form

$$\frac{\phi(r_b, z_b)\sin\theta_b}{2} = \int_{\partial\Delta} \frac{\partial(\phi(r,z)\sin\theta)}{\partial n_{r,z}} G(r_b, \theta_b, z_b, r, \theta, z)\,\mathrm{d}s_{r,z} - \int_{\partial\Delta} \frac{\partial G(r_b, \theta_b, z_b, r, \theta, z)}{\partial n_{r,z}} \phi(r,z)\sin\theta\,\mathrm{d}s_{r,z} \tag{43}$$

Since the problem is axisymmetric, we can choose an arbitrary value for θ_b in the above equation. For $\theta_b = \frac{\pi}{2}$ we get

$$\phi(r_b, z_b) = \frac{1}{2\pi}\int_{\partial\Omega}\left(\frac{\partial\phi(r,z)}{\partial n_x} g(r,z,r_b,z_b) - \phi(r,z)\tilde{g}(r,z,r_b,z_b)\right)\mathrm{d}s_{r,z} \tag{44}$$

where

$$g(r,z,r_b,z_b) = 4\pi\int_0^{2\pi} G\left(r,\theta,z,r_b,\frac{\pi}{2},z_b\right)\sin\theta\,\mathrm{d}\theta \tag{45}$$

$$\tilde{g}(r,z,r_b,z_b) = 4\pi\int_0^{2\pi} \frac{\partial G(r,\theta,z,r_b,\frac{\pi}{2},z_b)}{\partial n_x}\sin\theta\,\mathrm{d}\theta \tag{46}$$

The integrands in (45) and (46) have an elementary expression in terms of r, r_b, z, z_b, θ and $\mathbf{n}$. However, the integrals themselves are of elliptic type and cannot be expressed in an elementary way. Moreover, they involve multidimensional singular integrals and their numerical evaluation is difficult. Such an evaluation can be found in the paper by Hamdi and Mebarek (1984). We opted for a different approach, which consisted in removing the singularity by integrating the singular parts exactly and performing the integration of the regular functions numerically. This gave rise to challenging numerical problems which are beyond the scope of this paper.

Equations (44) and (36) give rise to a finite-element approximation. A triangular mesh τ_h is built over Ω. The mesh on the boundary $\partial\Omega$ is induced by τ_h. Since the normal derivative of ϕ is not continuous on $\partial\Omega$, we introduce a new variable

$$\lambda = \frac{\nu}{r}\frac{\partial(r\phi)}{\partial n} \tag{47}$$

which is continuous on $\partial\Omega$ according to (40). To approximate ϕ, we use standard $\mathbf{P}_1$ elements inside Ω, while $\mathbf{P}_0$ elements are used to approximate λ on $\partial\Omega$. We thus obtain a linear system where the unknowns are the values of ϕ at the mesh nodes and the values of λ on the boundary edges. Accordingly, we obtain a boundary-element-finite-element model which was implemented in an eddy-current computation code.

4. Hysteresis Model

In the case of ferromagnetic materials, heat is generated not only through the Joule effect, but also by losses due to hysteresis. Our aim was to implement a simple model which would account for hysteresis and would be efficient from a computational point

of view. Obviously, considering hysteresis on a microscopic scale was not an acceptable solution and we had to opt for a macroscopic model. This model was developed in the Electricity Department of the Swiss Federal Institute of Technology by M. Jufer and M.M. Radulescu (see Jufer and Radulescu, 1994).

In non-ferromagnetic materials, the relation between the magnetic field $\mathbf{H}$ and the magnetic induction $\mathbf{B}$ is given by (4). A good approximation for hysteresis is to consider a dependency between $\mathbf{H}$ and $\mathbf{B}$ in the form

$$\mathbf{H}(t) = \nu \mathbf{B}(t + t_d) \tag{48}$$

where t_d denotes a delay due to hysteresis. On account of (6) and (7), eqn. (48) can be rewritten as

$$\mathbf{H} e^{i\omega t} = \nu \mathbf{B} e^{i\omega(t+t_d)} \tag{49}$$

where $\mathbf{H}$ and $\mathbf{B}$ do not depend on time t. If we define $\tilde{\nu} = \nu e^{i\omega t_d}$, relation (4) can be replaced by

$$\mathbf{H} = \tilde{\nu} \mathbf{B} \tag{50}$$

where $\tilde{\nu}$ is a complex equivalent magnetic reluctivity. The rest of the model does not change. The source term for the heat equation is therefore given by

$$\eta = q_1 + q_2 \tag{51}$$

where

$$q_1 = \frac{1}{2} \omega^2 \sigma |\phi|^2 \tag{52}$$

corresponds to Joule's power losses, while

$$q_2 = \frac{1}{2} \tilde{\nu} \omega |\mathbf{B}|^2 \tag{53}$$

accounts for power dissipated by hysteresis. If the inductor moves vertically with respect to the workpieces at a speed v, additional heat is generated. The corresponding source term is

$$q_3 = \frac{1}{2} v^2 \sigma \left| \frac{\partial \phi}{\partial \sigma} \right|^2 \tag{54}$$

However, in industrial induction heating applications, the speed v is not high enough to make this term significant. Details of this part of the work can by found in the report by Jufer and Radulescu (1994).

5. Other Computations

The source term obtained from the electromagnetic solver is included into a finite-element heat equation solver. Based on an enthalpy formulation, this solver encompasses a number of advanced features, such as the computation of look factors for radiation study and the possibility of including heat transfer conditions of any kind. The latter feature is particularly necessary for the simulation of water cooling during quenching. An attempt to solve the Navier-Stokes equation describing the water flow on the surface, and solving the heat equation for water would give rise to a very difficult problem. Alternatively, we opted for the use of an equivalent heat transfer coefficient. Its value for different quenching conditions and liquids is deduced by inverse methods from the results of experiments.

During quenching, steels undergo solid-state phase transformations which affect their physical properties and generate latent heat. Taking into account these transformations is essential for obtaining correct simulation results. Therefore, the induction heating simulation software was equipped with a module computing microstucture changes, developed in the Material Science Department of the Swiss Federal Institute of Technology by Michel Rappaz and Alain Jacot (see Jacot *et al.* 1996). The laws that describe phase changes between different microstructures in steels (such as ferrite, perlite, austenite and martensite) take into account, generally speaking, the temperatures reached and the heating rate. On the other hand, the generated latent heat is included as a source term into the heat equation. A detailed account of this work can be found in the paper by Jacot *et al.* (1996).

The structure of the whole simulation software is represented in Fig. 3. Its operation can be described as follows. An electromagnetic computation is performed for given initial conditions. Its results are assumed to be valid for a short timestep τ, as long as the electromagnetic properties of the conductors have not changed too much, i.e. as long as there is no large increase in temperature, and as long as the displacement of the inductors is small. Then the heat equation is solved for the timestep τ, providing a new value of the temperature field. Next, the microstructure module computes the steady-state phase changes. The possible latent heat influences the solution to the heat equation. In this case, the solution to both the heat and microstructure modules is obtained in an iterative way. The data regarding the temperature, the microstructures and the magnetic field are then used to update the values of the physical properties of the inductors and the workpieces. If the inductors move, their position after the timestep τ is then computed. After performing all these steps, we are ready for a new electromagnetic computation, and the whole process is repeated as many times as necessary. The software presented here was provided with a user-friendly input-output interface and is now used in industrial practice.

6. Sample Results and Comparison with Experimental Data

A stream heating experiment was carried out at the laboratories of the Amysa Yverdon SA company. An inductor was moved downwards along a cylindrical workpiece made of ferromagnetic ck45 steel. Only the heating effect was investigated; no

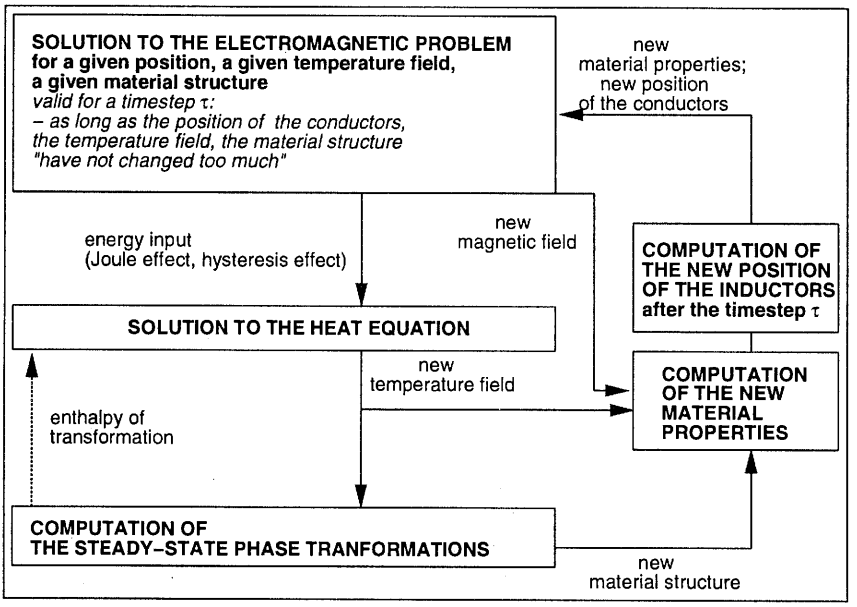

Fig. 3. The structure of the simulation software.

quenching was performed. (For results involving quenching, refer to the paper by Jacot *et al.* (1996).) The characteristics of the experiment are shown in Fig. 4. Several thermocouples were arranged inside the workpiece. Their locations are represented in Fig. 5. A numerical simulation was performed according to the same specifications. Figure 4 shows the isotherms at different moments, obtained by numerical simulations. Figure 7 shows a comparison of temperatures at the measurement points between the experiment and numerical simulation. It can be observed that the measurement of temperatures is not easy in the conditions of the experiment presented here. Moreover, the size of the thermocouple is about 0.5 mm, while temperature gradients in the workpiece can reach magnitudes of 100 Kelvins per mm. Therefore, it can be concluded that discrepancies between the measurement and experiment observed in Fig. 5 are of the order of experimental error.

Acknowledgements

The authors wish to thank Mr A. Jacot and Prof. M. Rappaz from the Material Science Department of the Swiss Federal Institute of Technology, Prof. M. Jufer and Dr. M.M. Radulescu from the Electricity Department of the Swiss Federal Institute of Technology, and Dr D. Mari from the company Amysa Yverdon SA for their contribution to this work and their valuable comments.

The authors also wish to express their gratitude to Prof. A.A. Jaecklin for his continuous support, encouragement and advice.

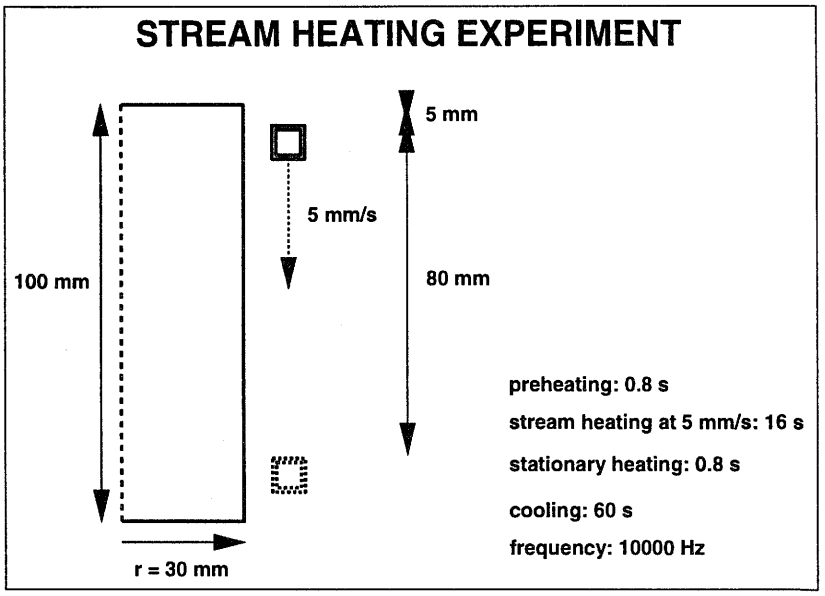

Fig. 4. The stream heating experiment.

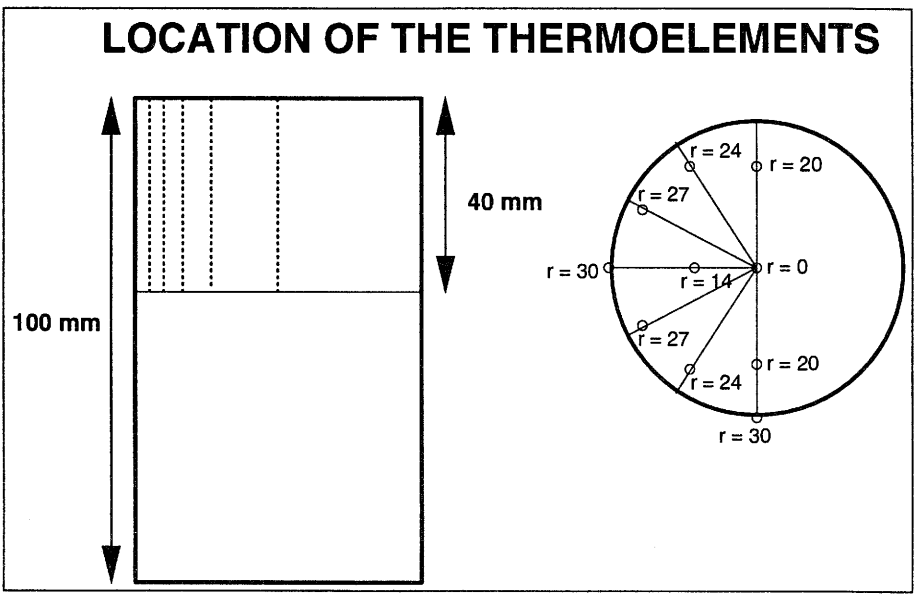

Fig. 5. Location of the thermoelements.

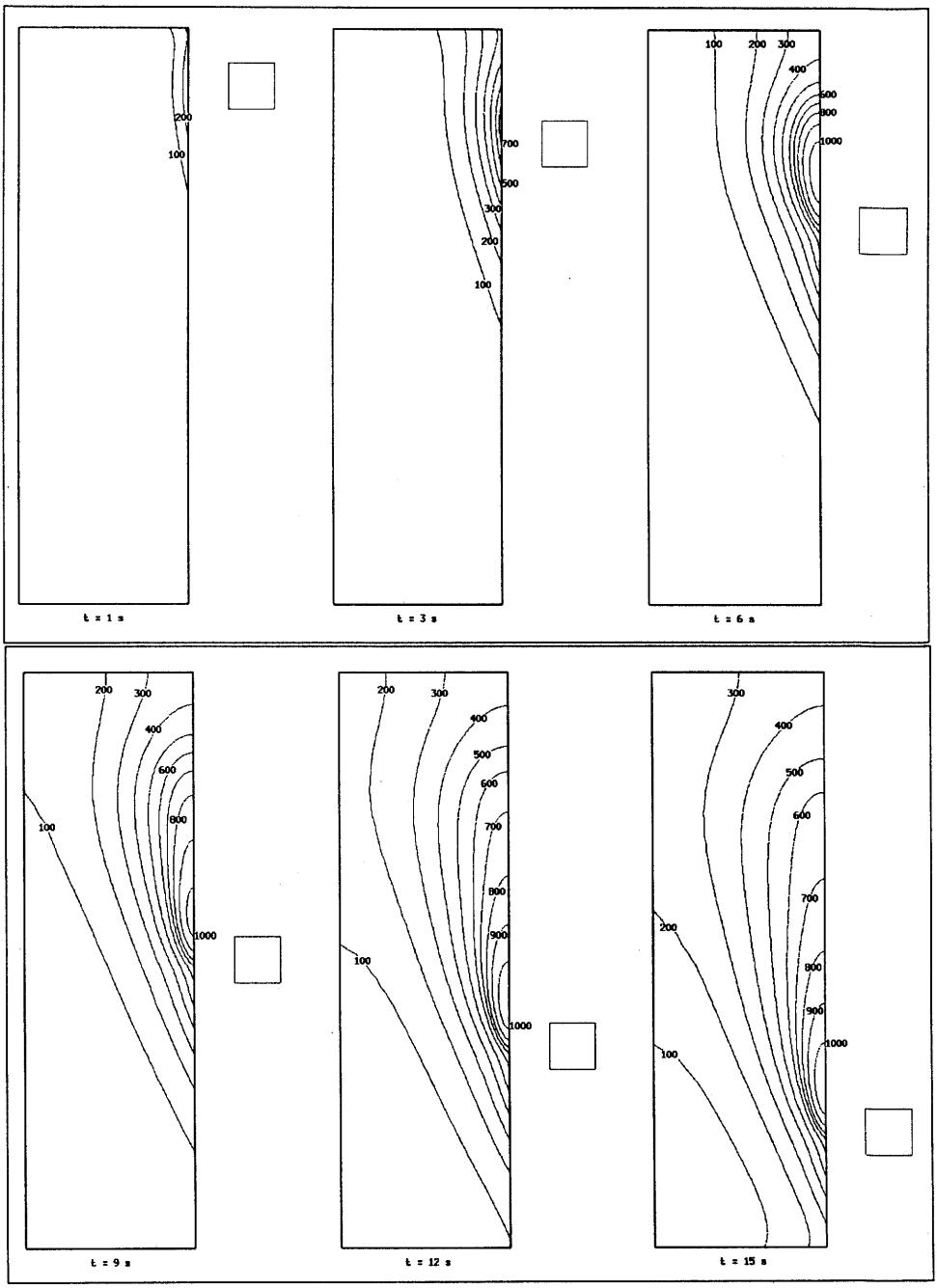

Fig. 6. Isotherms during heating.

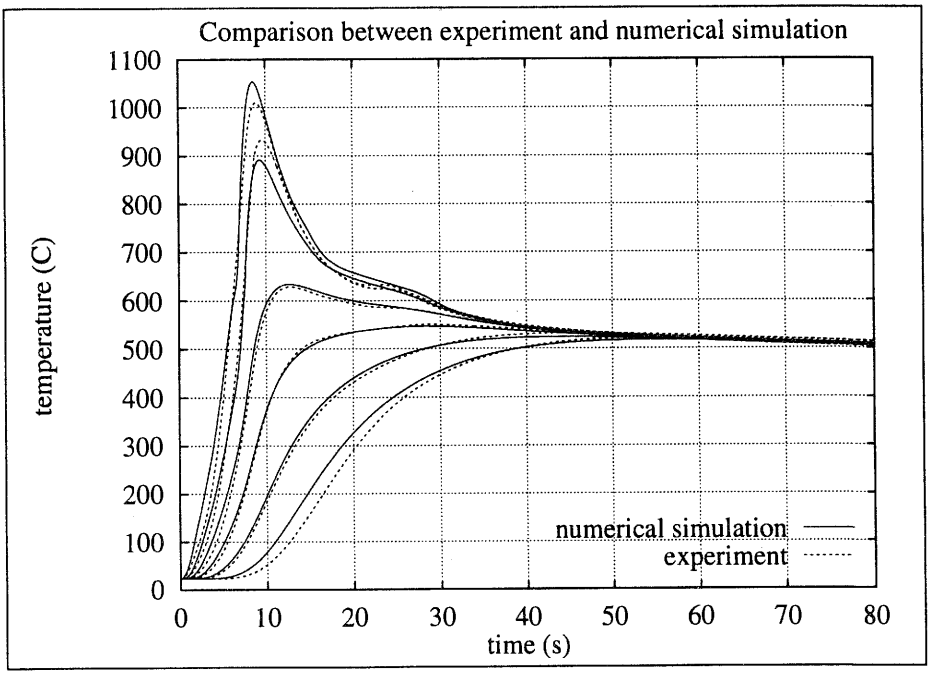

Fig. 7. Comparison between experiment and numerical simulation.

References

Jacot A., Świerkosz M., Rappaz J., Rappaz M., and Mari D. (1996): *Modelling of electromagnetic heating, cooling and phase transformations during surface hardening of steels.* — Proc. *Mecamat'95*, La Bresse, France, Journal de Physique IV, (in print).

Jufer M. and Radulescu M.M. (1994): *Inclusion of Magnetic Hysteresis Losses in the Modelling of Induction Heating for Axisymmetric Geometries.* — Internal Report, LEME EPFL, Lausanne, Switzerland.

Dautray R. and Lions J.-L. (1988): *Analyse mathématique et calcul numérique pour les sciences et les techniques.* — Paris: Masson.

Nédélec J.C. (1977): *Approximation des équations intégrales en mécanique et en physique.* — Cours du Centre de Mathématiques Appliquées, The Ecole Polytechnique in Paris.

Hamdi M.-A. and Mebarek L. (1984): *Rayonnement des structures à géométrie axisymétrique.* — Proc. *9e Colloque d'Acoustique Aéronautique*, Compiègne, France, pp.132–146.